

## Measurement of the Pfirsch-Schlüter and Bootstrap Currents in a Stellarator

J. D. Treffert and J. L. Shohet

*Torsatron/Stellarator Laboratory, University of Wisconsin, Madison, Wisconsin 53706*

and

H. L. Berk

*Institute for Fusion Studies, University of Texas, Austin, Texas 78712*  
(Received 27 December 1982; revised manuscript received 11 September 1984)

The Proto-Cleo stellarator has parameters that are sufficient to generate values of equilibrium (Pfirsch-Schlüter) currents and diffusion-driven (bootstrap) currents of magnitude large enough to permit local measurement of these currents with probes inserted in the plasma. Symmetric and antisymmetric components of the current yielded minor radial profiles that are consistent in magnitude, direction, and scaling with predicted values of Pfirsch-Schlüter and bootstrap currents.

PACS numbers: 52.55.Gb, 52.25.Fi

Considerable attention<sup>1-3</sup> has been given to the study of magnetohydrodynamical equilibrium and bootstrap currents in toroidal devices. A bidirectional current which flows parallel to the magnetic field (Pfirsch-Schlüter current) is predicted to limit beta by causing an outward shift. A unidirectional parallel diffusion-driven ("bootstrap") toroidal current is predicted to be the minimum net parallel current in toroidal devices.<sup>1</sup> An experimental investigation of the radial distribution of such currents in the Proto-Cleo stellarator has been conducted. This Letter presents results which indicate that both bidirectional and unidirectional currents are present. The magnitudes, profiles, and directions of these currents are consistent with theoretical predictions for the Pfirsch-Schlüter and bootstrap currents, respectively. This is the first direct measurement of such currents in stellarators.

Proto-Cleo is a small ( $R=40$  cm,  $r_{\text{plasma}}=4.5$  cm,  $B_0=3$  kG)  $l=3,7$  field period classical stellarator. Plasma is gun injected toroidally at the separatrix. The plasma parameters ( $n=1 \times 10^{12}$  cm<sup>-3</sup>,  $T_e=10$  eV,  $T_i=50$  eV) are sufficiently high so that the local currents should be observable, and sufficiently low to allow the use of probes. No externally driven current is present.

Local currents are measured with a small "paddle" probe, shown in Fig. 1. It consists of two parallel platinum electrodes, closely matched in area and insulated from each other. The electrodes are connected via low-impedance sampling resistors to the vacuum tank. The values of the sampling resistors are adjusted so that the output voltage/ampere is the same for both electrodes and when the probe is rotated 180°. The measured directed currents were at least 4 times smaller than the thermal

currents. Extensive calibration was required to ensure that the probe could accurately measure the directed currents. Density and temperature fluctuations were very low and did not affect the measurements.

Local currents were also measured with a miniature Rogowski coil, which has a major radius of 5 mm and a minor radius of 1 mm. It has a 2400-turn main coil and a 10-turn compensating coil used to correct coil winding errors. Total plasma current was monitored with a larger Rogowski coil. Measurements made with the miniature Rogowski coil are consistent with those made with the paddle probe. The large Rogowski measurements agree with the total current based on the radial profile

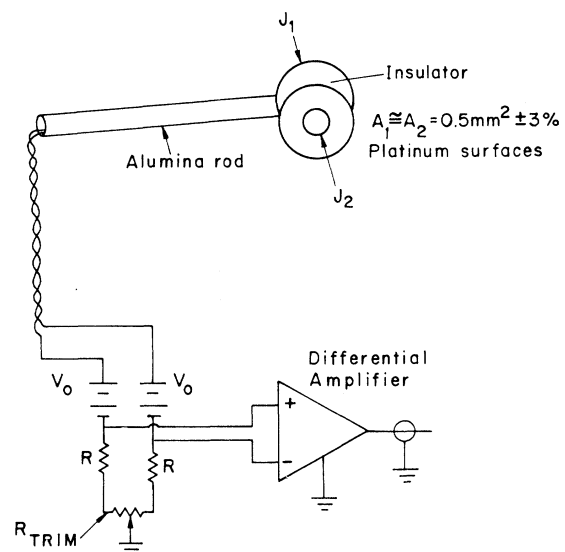


FIG. 1. Paddle probe.

measurements. Integrated line density was measured with a microwave interferometer.

Probe data for which the microwave interferometer gave comparable line density evolution were evaluated. If the line density of two shots matched well, the probe-measured currents matched well also. The plasma density profile shape has been shown<sup>4</sup> to remain relatively constant as the density decays. The probe-induced reduction in line density was small at points far from the probe. Several radial probe scans were made during each data collection series, and a total of 20–30 shots were taken at each position. Some measurements were made at a different toroidal angle, one field period away. These were consistent.

Local electron temperatures and densities were obtained with swept floating double Langmuir probes or ion-saturation probes normalized to the line density. Line-averaged ion temperatures were obtained with a swept Fabry-Perot interferometer.

Plasma behavior in the first 100–300  $\mu\text{sec}$  after injection is variable, but can be characterized by unidirectional currents, peaked at the outer edge of the plasma, having magnitudes of 5 A/cm<sup>2</sup>. In some cases the buildup of current is preceded by 20–30-kHz oscillations. For times greater than 400  $\mu\text{sec}$  after injection, the currents are reproducible to within 10%. Figure 2 shows the time evolution of the toroidal electron current profiles in this time region. No significant change in the profiles was observed after the first 400  $\mu\text{sec}$  when the gun injection direction was reversed.

Estimates of currents induced by the time variation of the main field (less than 5% over a shot) predict that any such currents should be several orders of magnitude less than the measured current. No change in direction of the current was observed in the presence of rising or falling main-field strength.

The current reverses directions on opposite sides of the magnetic axis. This profile can be viewed as the superposition of a unidirectional (symmetric) and a bidirectional (antisymmetric) current. The bidirectional current is the Pfirsch-Schlüter current. This current is calculated by imposition of the condition  $\nabla \cdot \vec{j} = 0$  together with the equilibrium defined by  $\vec{j} \times \vec{B} = \nabla p$ . If we take

$$\vec{j} = \vec{j}_{\parallel} + \vec{j}_{\perp} = \vec{j}_{\text{P-S}} + \vec{j}_{\text{eq}},$$

then we obtain the condition<sup>2</sup>

$$\vec{j} = (\partial p / \partial \alpha) [h \vec{B} + (\vec{B} \times \nabla \alpha / B^2)], \quad (1)$$

where, from  $\nabla \cdot \vec{j} = 0$ , we obtain

$$\vec{B} \cdot \nabla h = (\vec{B} \times \nabla \alpha / B^2) \cdot (\nabla B^2 / B^2). \quad (2)$$

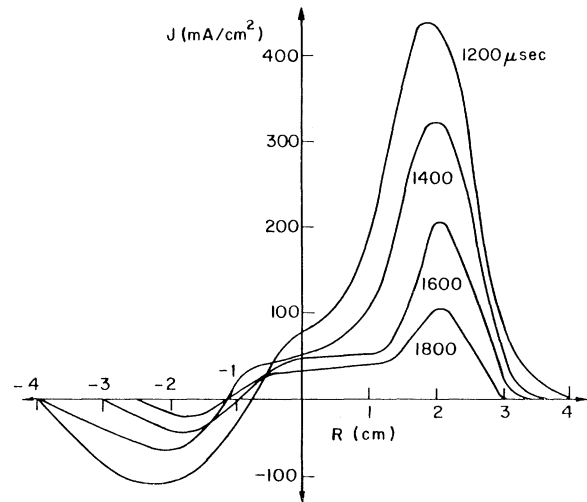


FIG. 2. Toroidal electron current 1200–1800 msec after injection.

Thus,  $h(s) = h(0) + h_1(s)$ , where

$$h_1(s) = + \int_0^s \frac{\vec{B} \times \nabla \alpha}{B^2} \frac{\nabla B^2}{B^2} \frac{dl}{B}, \quad (3)$$

$\alpha$  is a Clebsch coordinate and  $dl$  is an element of arc length along  $B$ . If a simple Ohm's law,  $\vec{E} = -\nabla \phi = \eta \vec{j}$ , is assumed, where  $\eta$  is the resistivity, then, because of the uniqueness of  $\phi$ , we obtain the condition

$$h(0) = - \int_{-\infty}^{\infty} h_1 B dl / \int_{-\infty}^{\infty} B dl. \quad (4)$$

A code which evaluates (3) in a convenient coordinate system for arbitrary fields has been developed.<sup>5</sup> With use of the actual vacuum fields for Proto-Cleo, this code has been used to obtain the Pfirsch-Schlüter current at the measurement site.

To lowest order in an inverse aspect ratio expansion Eq. (1) yields<sup>2</sup>

$$\vec{j}_{\text{P-S}} = -(2/\epsilon B) (dp/dr) \cos(\theta) \hat{\phi}, \quad (5)$$

where  $\theta$  and  $\phi$  are the poloidal and toroidal angles.  $\epsilon$  is the rotational transform divided by  $2\pi$ . In this limit, the Pfirsch-Schlüter current is of opposite sign at the two intersections of each magnetic surface with the horizontal midplane. By similar reasoning, the measured toroidal electron currents were decomposed, in flux coordinates, into symmetric and antisymmetric components and transformed back into real space. Figure 3 shows the measured toroidal electron current profile, 1.4 msec after injection, decomposed as defined above. Since the ion current, measured by the paddle probe, is an order of magnitude less than the electron current, it can be assumed that charge neutrali-

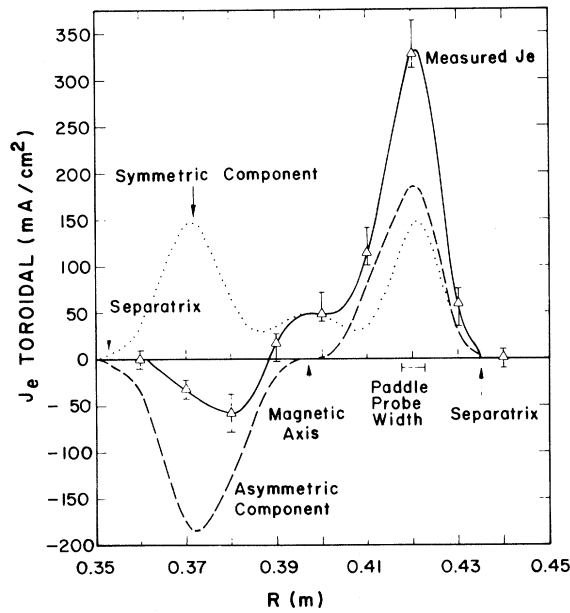


FIG. 3. Toroidal currents as a function of major radius.

zation is accomplished by the electrons, and the total pressure may be used in evaluation of the electron current.

Figure 4 shows the numerically evaluated

Pfirsch-Schlüter current profile and the antisymmetric (in flux coordinates) component of the measured current. The peak total pressure assumed in the calculation of Fig. 4 was  $1.45 \times 10^{13} \text{ eV cm}^{-3}$ . Experimental measurements place the total pressure at  $1.45 \times 10^{13} \text{ eV cm}^{-3} \pm 30\%$ . Thus, the antisymmetric component of the measured current differs from the numerically evaluated Pfirsch-Schlüter current by less than 30%.

The symmetric component of the toroidal current agrees with the diffusion-driven or bootstrap current. For a collisional toroidal axisymmetric plasma in quasistationary ambipolar equilibrium, the bootstrap current is given by<sup>3</sup>

$$j_{bs} = -2(dp/dr)\epsilon f = -|j_{p-s}|_{\theta=0}\epsilon f, \quad (6)$$

where

$$f = \frac{v_a(v_a + U_{ni})(U_{ni} - U_{ne})}{D[v_a + U_{ni} + s(U_{ni} - U_{ne})]}$$

and

$$D = v_a(v_a + U_{ne}) - c_s^2 \epsilon^2 \tau^2.$$

$v_a$  is the ambipolar plasma rotation velocity,  $\epsilon$  is the inverse aspect ratio,  $U_{ne}$  and  $U_{ni}$  are the electron and ion drift velocities,  $c_s$  is the sound speed, and  $s$

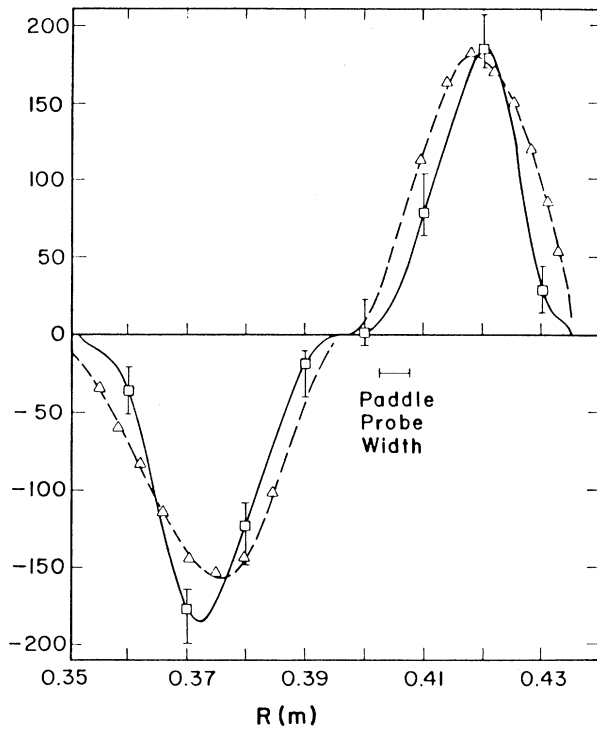
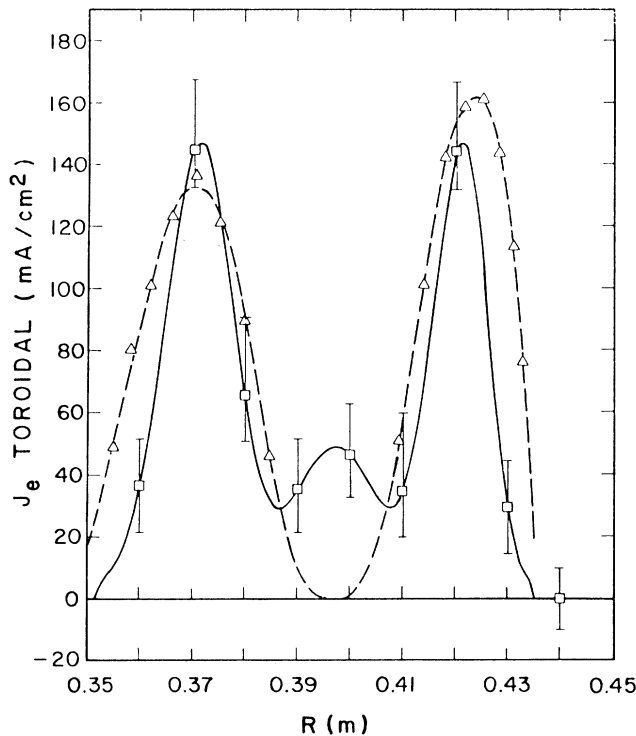


FIG. 4. Experimental measurements (solid lines) and theoretical models (dashed lines) for symmetric currents (left graph) and antisymmetric currents (right graph) as a function of major radius.

is a constant equal to 0.71. The quasistable rotation velocities satisfy<sup>3</sup>

$$\left( \frac{v_a(v_a + U_{ni})U_{ne}}{D(U_{ni} - U_{ne})} + s \right) \left( \frac{v_n + U_{ni}}{U_{ni} - U_{ne}} + s \right) + \alpha = 0, \quad (7)$$

where  $\alpha = \eta \chi_{\parallel e}^2 / kT_e$  and  $\chi_{\parallel e}$  is the parallel electron thermal conductivity. The roots of (7) were obtained and substituted into (6). Only one quasistationary solution was in the proper direction to account for the current observed in Proto-Cleo. The function  $f$  is constant to within 10% for minor radii from 0.75 to 4.0 cm. Expression (6) is then used to obtain an estimate for the bootstrap current. Figure 4 shows the calculated midplane bootstrap current profile and the symmetric component of the measured current. In Fig. 4,  $f$  was assumed to be 14.5. Measured  $T_e$  and  $T_i$  place  $f$  at  $14.5 \pm 15\%$ . Thus, the measured symmetric electron current differs from the bootstrap current predicted by this model by less than 45%.

This model does not take helical diffusion into account. However, toroidal diffusion should dominate in the regime of collisionality valid here. Also, it was again assumed that the electrons respond to a force proportional to the total pressure gradient. A diffusion model similar to that used above, but including the effects of ion viscosity,<sup>6</sup> predicts that this assumption is true for the steady state, and also predicts oscillations consistent with those observed during the first 100–300  $\mu\text{sec}$  of the discharge. It also predicts electric fields which agree with rough estimates for Proto-Cleo based on measurements of the floating potential.<sup>7</sup>

The bidirectional current exhibited a rough  $1/B$  dependence. This is consistent with magnetohydrodynamical theory. For times greater than 1.0 msec, both the peak bidirectional and unidirectional currents scale linearly with pressure, as would be expected, since the pressure profile remains constant. However, the relatively small on-axis current, not predicted by the bootstrap model, has a much different time (pressure) dependence and may be due to other effects, including residual injection currents.

The authors would like to acknowledge several helpful conversations with W. N. G. Hitchon. This work was supported by the U.S. Department of Energy under Contract No. DE-AC02-84ER53166 and No. DE-FG05-80ET53088 and by the National Science Foundation under Grant No. ECS-8206027.

<sup>1</sup>T. E. Stringer, in *Proceedings of the Third International Symposium on Toroidal Plasma Confinement, Garching, Germany, 1973* (Max-Planck-Institut für Plasmaphysik, Garching, Germany, 1973).

<sup>2</sup>L. S. Solovév and V. D. Shafronov, in *Reviews of Plasma Physics*, edited by M. A. Leontovich (Plenum, New York, 1975), Vol. 5, p. 142.

<sup>3</sup>T. E. Stringer, *Plasma Phys.* **14**, 1063 (1972).

<sup>4</sup>D. J. Hoffman and J. L. Shohet, *Nucl. Fusion* **23**, 87 (1983).

<sup>5</sup>H. L. Berk, M. N. Rosenbluth, and J. L. Shohet, *Phys. Fluids* **26**, 2616 (1983).

<sup>6</sup>E. Bowers and N. K. Winsor, *Phys. Fluids* **14**, 2203 (1971).

<sup>7</sup>D. J. Hoffman, J. N. Talmadge, and J. L. Shohet, *Nucl. Fusion* **21**, 1330 (1981).